JOURNAL OF GEOPHYSICAL RESEARCH, VOL. 88, NO. A11, PAGES 8959–8970, NOVEMBER 1, 1983

A Survey of Electrostatic Waves in Saturn's Magnetosphere

W. S. KURTH,[1] F. L. SCARF,[2] D. A. GURNETT,[1] AND D. D. BARBOSA[3]

The Voyager 1 and 2 plasma wave instruments have provided initial observations of electrostatic waves in Saturn's magnetosphere. In general, the emissions at Saturn are similar to those found at earth and Jupiter, although there are significant differences in some of the detailed characteristics. In this paper we present an overview of the various types of electrostatic waves in the Saturnian magnetosphere, including Langmuir waves and electron cyclotron harmonic emissions. We shall summarize the temporal and spectral character, amplitude, and regions of occurrence for the various classes of emissions. These characteristics are compared with those of the terrestrial and Jovian counterparts with the goal of understanding how major differences in the magnetospheric configuration might contribute to the observed differences. Finally, we use the theory of electron cyclotron harmonic emissions to try to gain an insight into the electron distributions and possible wave-particle interactions in Saturn's magnetosphere.

1. INTRODUCTION

Some of the most intense plasma waves observable in a planetary magnetosphere are electrostatic waves that are the result of plasma instabilities related to sources of free energy in the electron distribution functions such as a loss-cone or bump on tail distribution. These waves are important in the study of the physics of planetary magnetospheres for several reasons. In some cases (for example, electron cyclotron harmonic emissions), the waves may interact strongly with trapped energetic electrons and pitch angle scatter them into the loss cone and, hence, be an important factor in the energy budget of the magnetosphere. In other cases, they may be of significant diagnostic value, providing an accurate measure of the plasma density as in the case of Langmuir waves. Electrostatic waves may also be the source of freely propagating radio emissions that allow the study of the magnetosphere via remote sensing techniques. In any case, the presence of various electrostatic plasma wave modes implies the presence of certain classes of distribution functions, thereby providing information that can yield some insight into dynamical processes within the magnetosphere.

The first evidence for electrostatic waves in the Saturnian magnetosphere was given by *Gurnett et al.* [1981*a*], who reported electron plasma oscillations at a distance of about 7 R_S on the Voyager 1 inbound leg and a series of banded emissions known as electron cyclotron harmonic emissions or $(n + 1/2)f_g$ bands where n is an integer and f_g is the electron gyrofrequency. The $(n + 1/2)f_g$ bands were observed on the Voyager 1 outbound leg inside ~ 7 R_S. Gurnett et al. also reported observing a special $(n + 1/2)f_g$ band at higher harmonics that is generally believed to be near the upper hybrid resonance frequency, f_{UHR}, defined by $f_{UHR} = \sqrt{f_p^2 + f_g^2}$, where f_p is the electron plasma frequency.

Pedersen et al. [1981] elaborated further on the electrostatic $(n + 1/2)f_g$ and UHR bands detected near the Voyager 1 periapsis by the planetary radio astronomy receiver. They used the presence of the upper hybrid emissions to deduce a plasma frequency and, hence, electron density profile (since $f_p = 8980\sqrt{n_e}$ where f_p is in Hz and n_e is the density in electrons cm^{-3}). Pedersen et al. inferred from the presence of the $(n + 1/2)f_g$ waves that the local plasma consisted of a mixture of relatively cold and hot magnetospheric plasmas.

The Voyager 2 encounter offered a second look at electrostatic waves in Saturn's magnetosphere. *Scarf et al.* [1982] again reported $(n + 1/2)f_g$ emissions throughout the inner magnetosphere ($R \lesssim 8$ R_S). The emissions were primarily observed in the first ($n = 1$) band and in the band near f_{UHR}. High resolution frequency-time spectrograms showed spectral and temporal structure within the $3f_g/2$ band. Scarf et al. suggested the presence of the electron cyclotron emissions implied electron precipitation into the atmosphere similar to the case at earth. Evidence was also shown for an intense but intermittent emission near 3.1 R_S at 2.7 kHz, a frequency thought to be the electron plasma frequency on the basis of plasma probe observations. They suggested the emission was the result of a field-aligned electron beam.

In this paper we present a survey of the electrostatic waves occurring in Saturn's magnetosphere based on the plasma wave observations obtained during both Voyager encounters with Saturn. However, we note here that the plasma wave receivers on the Voyager spacecraft [*Scarf and Gurnett*, 1977] have only an electric dipole antenna and no magnetic sensor, hence, we cannot directly determine whether an emission is electrostatic or electromagnetic. Instead, we rely on clues provided by the emission frequency and its relationship to the characteristic frequencies of the plasma, their temporal character since electrostatic waves are inherently more impulsive than most electromagnetic waves, and by analogy with terrestrial plasma waves.

Also, it should be noted that all the phenomena covered in this paper are waves whose primary interaction is with electrons. Low-frequency electrostatic modes such as ion cyclotron waves are not discussed herein, primarily because there is little or no direct, confirming evidence of their existence at this time. This statement is primarily the result of instrument limitations and should not be taken to mean that electrostatic ion modes are not present in the Saturnian magnetosphere. There are two reasons the low-frequency waves are difficult to identify with the Voyager plasma wave instrumentation. First, the low-frequency end of the spectrum (below about 100 Hz) is covered only by coarsely spaced filter channels that do not allow the identification of banded emissions such as ion cyclotron waves, hence, it is difficult to differentiate between these emissions and

[1]Department of Physics and Astronomy, University of Iowa, Iowa City, Iowa, 52242.
[2]Applied Technology Division, TRW Space and Technology Group, Redondo Beach, California, 90278.
[3]Institute of Geophysics and Planetary Physics, University of California, Los Angeles, California, 90024.

Paper number 3A0315.
0148-0227/83/003A-0315$05.00

ELF hiss or other phenomena. Second, the noise spectrum produced by the spacecraft is most intense below 1 kHz and is often spiky, making it very difficult in some cases to differentiate between true signals and interference. Identification of the low-frequency modes, then, will only be possible after a lengthy and careful analysis of the data and will not be attempted here.

In the next section we will give a thorough summary of the occurrence and spectral characteristics of Saturnian electrostatic waves. In the discussion section we will elaborate on the similarities and differences between the emissions observed at Saturn with those studied previously at the earth and Jupiter. Finally, we will draw upon our theoretical knowledge of the electron cyclotron harmonic waves in order to make inferences about the electron distribution function in various regions of the Saturnian magnetosphere.

2. Observations of Electrostatic Waves in Saturn's Magnetosphere

The majority of the electrostatic waves observed in the Saturnian magnetosphere are of the electron cyclotron harmonic or $(n + 1/2)f_g$ variety; hence, this section shall deal mainly with observations of this type of emission. Before discussing the electron cyclotron harmonic emissions, however, we shall discuss two other, less prominent phenomena which can be generally classified as Langmuir waves.

2.1 *Langmuir Waves*

Figure 1 shows plasma wave data from the Voyager 1 inbound pass in the dayside outer magnetosphere at a radial distance of 15.6 R_S. The upper panel shows data from the plasma wave spectrum analyzer. Here, peak and average electric field strengths are plotted on a logarithmic scale for each of nine frequency channels with the vertical range from one channel to the next higher corresponding to about 100 dB. The height of the solid black area is proportional to the average field strength measured in 24-s intervals and a line is plotted connecting the peak values for the same intervals. All times used herein are spacecraft event times (SCET). For most of the period shown the peak trace does not appear, indicating that the peak and average values are nearly identical. For the bursty emission between 5 and 10 kHz, however, the peak trace is often visible, hence, there is a significant difference between the peak and average field strengths.

The lower panel in Figure 1 is a frequency-time spectrogram obtained from the wideband receiver that shows the intensity of waves as a function of frequency (ordinate) and time (abscissa).

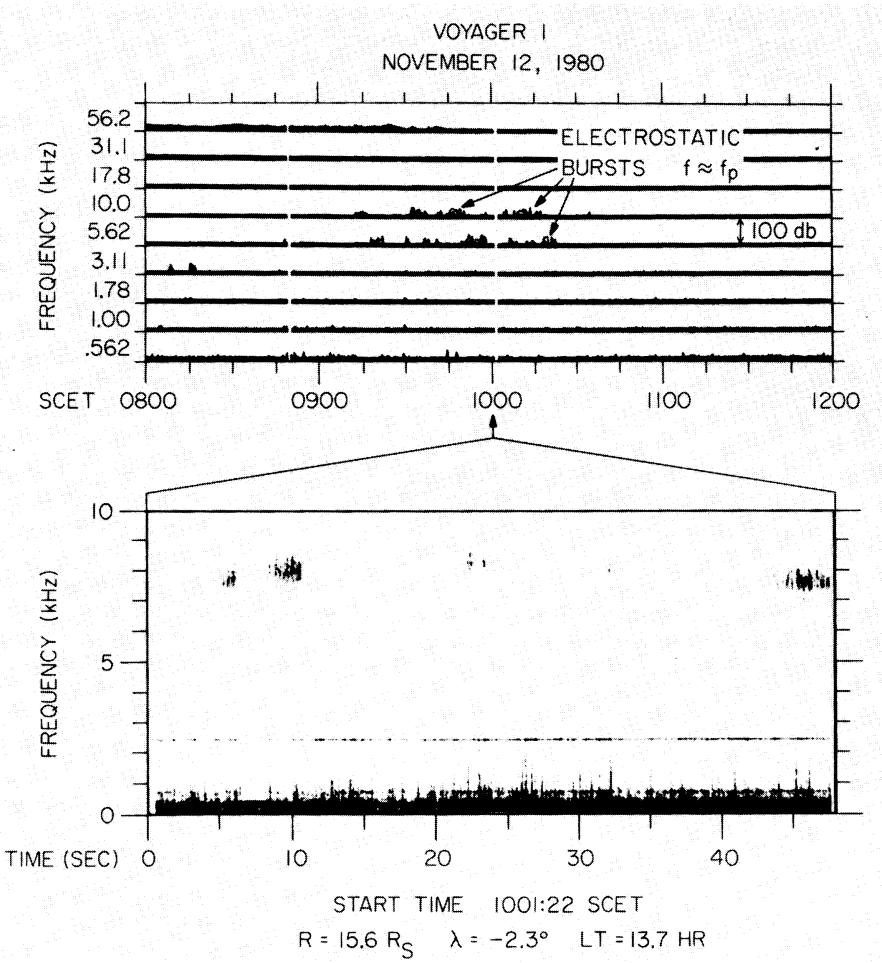

Fig. 1. In the upper panel evidence is shown for sporadic electrostatic bursts thought to be near f_p. A detailed frequency-time spectrogram in the lower panel shows the broadband nature of the bursts. Some of the bursts show a harmonic structure with frequency spacing of about 100 Hz. This spectral broadening and harmonic structure has led to the identification of these bursts as those generated by electrons in Landau resonance with a whistler mode wave such as chorus similar to emissions which have recently been discovered at earth.

The most intense waves are plotted as black on the spectrogram. Since the bottom panel contains only 48 s of data, the resolution (both temporal and spectral) is obviously much greater than that in the upper display. In the bottom panel it can be seen that the bursts near 8 kHz are extremely sporadic or bursty and have relatively large bandwidths, typically about 700 Hz. Figure 2 shows a 1.8-s average spectrum from the burst occurring about 9 s into the wideband frame shown in Figure 1. It is apparent from Figure 2 that the bursts have a bandwidth $\Delta f \approx 700$ Hz (full width at half maximum FWHM) and $\Delta f/f$ is about 10%.

On the basis of the spectrum analyzer data in Figure 1 (upper panel) we might identify the bursty emission between 5 and 10 kHz as Langmuir waves at the local electron plasma frequency or emissions at the upper hybrid resonance frequency. The 700-Hz bandwidth, however, immediately eliminates the UHR emissions as a possibility since the local gyrofrequency is about 280 Hz [*Ness et al.*, 1981] and a UHR band would be confined between successive harmonics of f_g. Similarly, if the electrostatic bursts in Figure 1 were the usual Langmuir waves, or electron plasma oscillations as they are sometimes called, we would not expect such a broadband emission. For example, *Gurnett et al.* [1981*c*] show Langmuir waves in the solar wind at 5.6 kHz (upstream from the Jovian bow shock) with $\Delta f/f \approx 1\%$. Nonlinear effects can broaden the line associated with the shock, but the frequency-time characteristics of the broadened line are not similar to those of the emissions seen in the lower panel of Figure 1. Hence, we shall use the term 'broadband' in referring to these emissions in the sense that they are much broader than expected for the usual Langmuir line.

In view of their broadband nature, the emissions shown in Figure 1 are very similar to electrostatic bursts that have recently been reported at the earth [*Reinleitner et al.*, 1982, 1983]. The emissions from the terrestrial magnetosphere are found primarily in the dayside outer magnetosphere at low latitudes and are characterized by broadband bursts centered at a frequency somewhat below the local electron plasma frequency. In some examples, the emissions show harmonic structure with the frequency spacing between the harmonics matching the frequency of a band of chorus often observed simultaneously in the terrestrial examples. Further investigation by Reinleitner et al. has shown the high-frequency electrostatic bursts are modulated at the chorus frequency. The modulation effect is most pronounced when the associated chorus is in the form of 'hooks,' i.e., having a frequency-time form that is narrowbanded and first falls rapidly in frequency, and then rapidly rises, all on a time scale of about a second.

The current explanation for the terrestrial emissions [*Reinleitner et al.*, 1983] is that the chorus is responsible for trapping electrons at the phase velocity of the whistler wave. The trapped electrons then excite an electrostatic instability through a type of two-stream instability called the resistive-medium instability. The theory predicts a shift to frequencies lower than f_p by an amount that Reinleitner et al. have shown to be related to the ratio between the beam velocity and the electron thermal speed. This downshift below the plasma frequency can range from a few percent to as much as 60%.

Comparison of the lower panel in Figure 1 with examples given by *Reinleitner et al.* [1982, 1983] shows the Saturnian bursts appear almost identical to the chorus-stimulated electrostatic waves observed in the earth's magnetosphere. In fact, there is some evidence of harmonic structures in the bursts with a frequency spacing of about 100 Hz that can be seen by careful

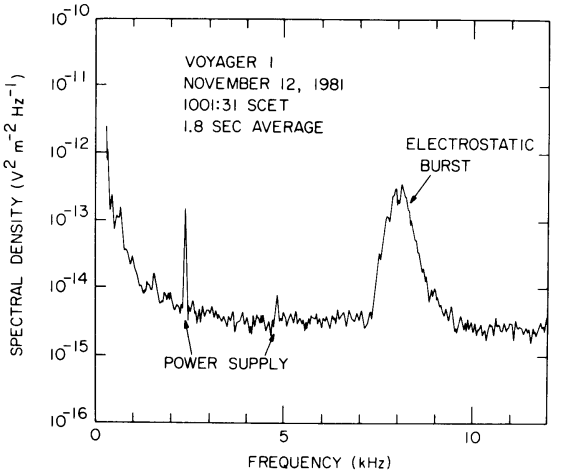

Fig. 2. A 1.8-second average spectrum taken from the spectrogram shown in the bottom panel of Figure 1. The frequency spread for the emission is obvious and differentiates this emission from the usual narrowband Langmuir waves.

inspection of the lower panel in Figure 1 and the spectrum in Figure 2. The gyrofrequency is about 280 Hz (based on a magnetic field strength of 10 nT [*Ness et al.*, 1981]) and, hence, the harmonic spacing would be consistent with a whistler-mode wave such as chorus at about $f_g/3$. The strongest signals shown in the lower panel at frequencies below about 300 Hz are interference tones from various spacecraft systems, such as the tape recorder, therefore, we are unable to confirm the presence of chorus at this time. On the other hand, if the theoretical explanation of *Reinleitner et al.* [1983] holds, the broad spectrum of the electrostatic bursts implies the existence of a low-frequency wave such as chorus.

Our identification of the bursts in Figure 1 as those studied by *Reinleitner et al.* [1982, 1983] is somewhat inconsistent with the measurements by the plasma probe on Voyager 1 (PLS). The electron density during this time interval (near 1000 SCET) as determined by the plasma science instrument is ~ 0.57 cm^{-3}, hence, $f_p = 8980\sqrt{n_e} = 6.8$ kHz (J. D. Scudder, private communication, 1982). This value is significantly below the frequency of the waves. We feel confident in our identification of the waves as electrostatic (and, hence, not at frequencies much above f_p) owing to their sporadic nature. We have considered the possibility that the waves were Doppler shifted to higher frequencies by the large corotational velocity of the plasma that is on the order of 150 km s^{-1} at the radial distance of the event in question. The maximum shift, however, even assuming the ideal geometry is only about 500 Hz (L. A. Reinleitner, private communication, 1982). This would not even offset the downshift in frequency predicted by *Reinleitner et al.* [1983] of about 600 Hz. Therefore, we do not believe Doppler shifts can explain the difference in the frequency of the waves and f_p obtained from the measured n_e. It may be possible that there is a significant fraction of very cold electrons that were not measured by the plasma probe.

The PLS observations offer some supporting evidence for the identification of the bursts in the upper panel of Figure 1 as being related to f_p, however, in that density variations implied by the burst frequency shifting between 5.62 kHz and 10.0 kHz are observed by PLS in the time interval 0915–1020 SCET (E. C. Sittler, Jr., private communication, 1983). While the frequency of the waves does not match the plasma frequency

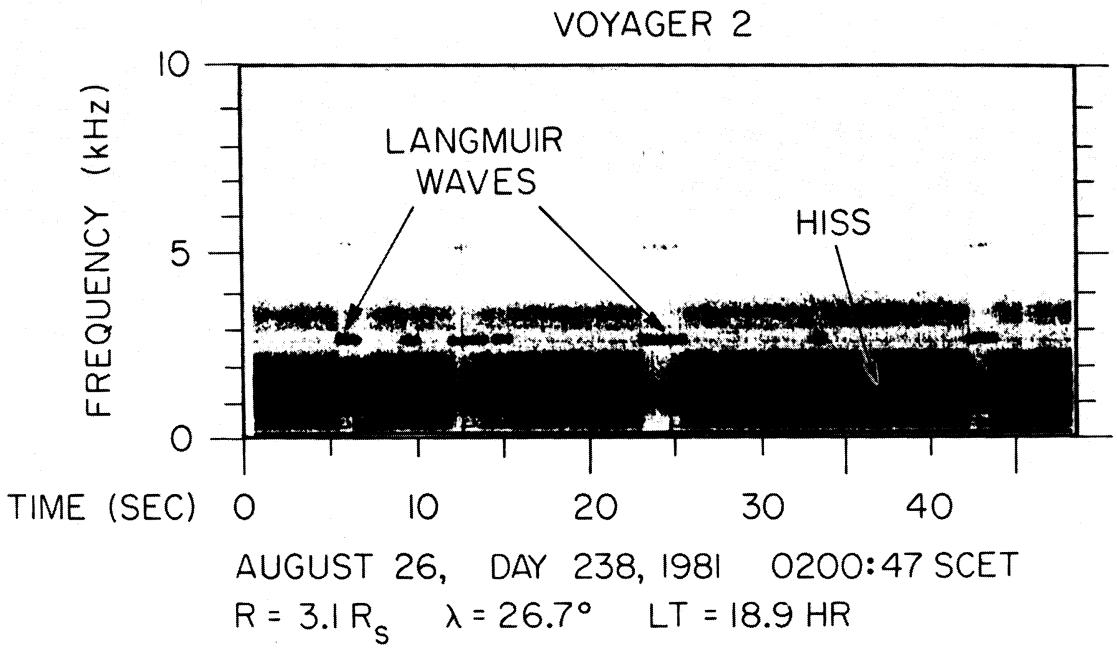

Fig. 3. The narrowband sporadic emissions at 2.7 kHz are identified as Langmuir waves on the basis of plasma probe measurements of the electron density. The electron gyrofrequency at this time was at a much higher frequency, 25.5 kHz.

derived from the PLS observations as noted above, the general trend of variation is seen, with the magnitude of density variations measured by PLS matching the magnitude of variations of the corresponding wave frequencies (keeping in mind that $n_e \propto f_p^2$). Hence, the emissions are apparently responding to the variation in density even though an explanation of the absolute frequency mismatch is not in hand.

Figure 3 is an example of Langmuir waves in the inner magnetosphere. These emissions are at the local electron plasma frequency based on measurements from the plasma science instrument [*Bridge et al.*, 1982] and are distinguishable from the emission shown in Figure 1 by their narrow bandwidth, about 90 Hz FWHM, hence, $\Delta f/f \approx 3\%$. Their intense, but sporadic presence differentiates these emissions from the narrowband electromagnetic radiation reported by *Gurnett et al.* [1981*a*, *b*] since the electromagnetic emissions are very persistent and show only very slow changes in amplitude with time. Figure 4 shows two 1.8-s average spectra taken from the spectrogram in Figure 3 at about 0201:05 SCET when the Langmuir waves were not present (left panel, Figure 4) and at about 0201:10 SCET during a burst of the Langmuir waves (right panel). The very intense, narrowband nature of the Langmuir waves is readily apparent in the spectrum shown in the right panel of Figure 4. The second and third harmonics of the Langmuir waves seen in Figure 3 are almost certainly an instrumental distortion of the extremely intense band (≈ 1 mV m^{-1}).

The Langmuir waves shown in Figure 3 are seen only rarely in the terrestrial magnetosphere and have not been reported at all in Jupiter's magnetosphere. In fact, as far as we know, *Gurnett et al.* [1983*c*] show the only other confirmed example of Langmuir waves within a planetary magnetosphere. While it is quite common to find narrowband emissions near f_p they are primarily Bernstein or $(n + 1/2)f_g$ waves near the upper hybrid resonance frequency [*Kurth et al.*, 1979] and, since $f_g \ll f_p$ in large regions of planetary magnetospheres, $f_p \approx f_{UHR}$. The Bernstein waves are polarized such that **k** (and therefore **E**) are oriented nearly perpendicular to the geomagnetic field. Langmuir waves, on the other hand, are polarized with $\mathbf{k} \| \mathbf{B}$. It is significant that for both the cases at the earth reported by *Gurnett et al.* [1983*c*] and that shown in Figure 3 f_p is less than f_g. The $(n + 1/2)f_g$ waves do not exist at frequencies below f_g (that is, in the $n = 0$ band), hence, the waves cannot be of the

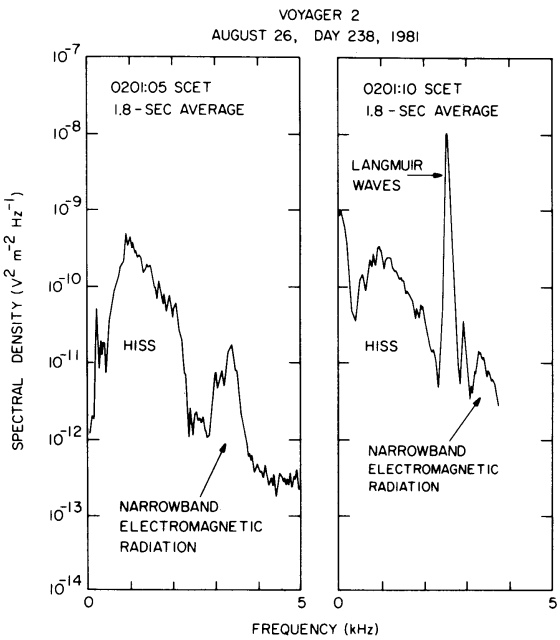

Fig. 4. 1.8-second average spectra taken from the data shown in Figure 3 when Langmuir waves are present (right panel) and absent (left panel). The Langmuir emission is extremely narrowbanded and has an integrated field strength of approximately 1 mV m^{-1}.

$(n + 1/2)f_g$ type. For the case shown in Figure 3, f_g is 25.5 kHz based on onboard magnetometer observations [*Ness et al.*, 1982]. As mentioned by *Scarf et al.* [1982] these waves suggest the presence of field-aligned electron beams. No evidence exists in the plasma probe data for a beam at this time; however, the instrument was in a very poor configuration to detect such a beam (J. D. Scudder, private communication, 1982).

2.2 *Electron Cyclotron Harmonic Emissions*

The most common electrostatic emissions in Saturn's magnetosphere are the electron cyclotron harmonic waves or $(n + 1/2)f_g$ bands. In fact, the low-latitude ($|\lambda| \lesssim 30°$) inner magnetosphere ($R \lesssim 8\ R_S$) seems to be characterized by a persistent emission between f_g and $2f_g$, commonly referred to as the 3/2 band. Figures 5 and 6 summarize the occurrence of the electron cyclotron emissions at Saturn on the basis of the Voyager 1 and 2 flybys, respectively. In both cases, data from several of the plasma wave receiver's spectrum analyzer channels have been plotted as a function of time and, in addition, plots of the radial distance and latitude as a function of time have been included in the upper panels. Superimposed on the data are curves showing the electron gyrofrequency [*Ness et al.*, 1981, 1982] and plasma frequency (E. C. Sittler, Jr., private communication, 1983) derived from the Voyager magnetometer and plasma science instruments, respectively. The f_p profiles are based on preliminary analyses of the PLS electron data and are subject to further analysis and comparison with the ion data.

The data in Figure 5 are from the Voyager 1 encounter and all were obtained after periapsis. Prior to about 0100 SCET the spacecraft had been in a region at high southern latitudes where the plasma frequency was well below the gyrofrequency, hence, the $(n + 1/2)f_g$ bands were not observed on the inbound leg. The 3/2 band is most prominent and the easiest to see in Figure 5, lying just above f_g starting at ~0200 and visible until about 0445 on day 318. The equator crossing occurred at about 0419 and there is a slight enhancement in the amplitude of the $n = 1$ band near this time. The bursty emissions after 0200 in the 31.1- and 56.2-kHz channels are thought to be higher harmonic emissions near the upper hybrid resonance frequency, consistent with density determinations by the plasma science investigation (E. C. Sittler, Jr., private communication, 1982). Additional $(n + 1/2)f_g$ emissions can be seen above the 3/2 band and below f_{UHR} but are weaker than the former bands and are barely detectable at the highest harmonics until f_{UHR} is reached.

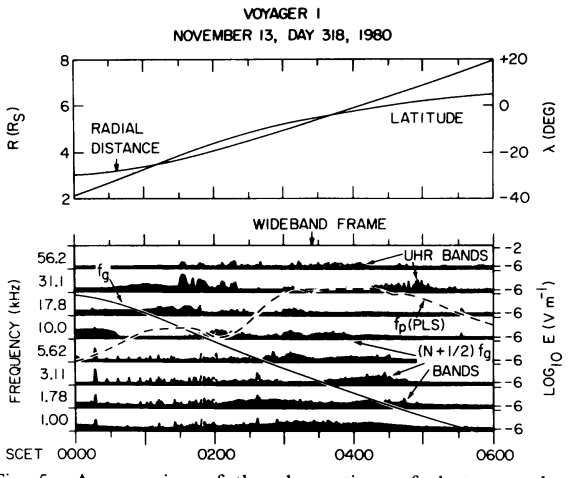

Fig. 5. An overview of the observations of electron cyclotron emissions observed by Voyager 1 on its outbound leg. The primary emission is the 3/2 band just above the f_g contour after 0200 SCET. The sporadic emissions after ~0200 in the 56.2- and 31.1-kHz channels are thought to be higher harmonic $(n + 1/2)f_g$ bands near f_{UHR}. Note that the electrostatic emissions were not observed on the inbound leg since $f_p < f_g$ for the interval before closest approach.

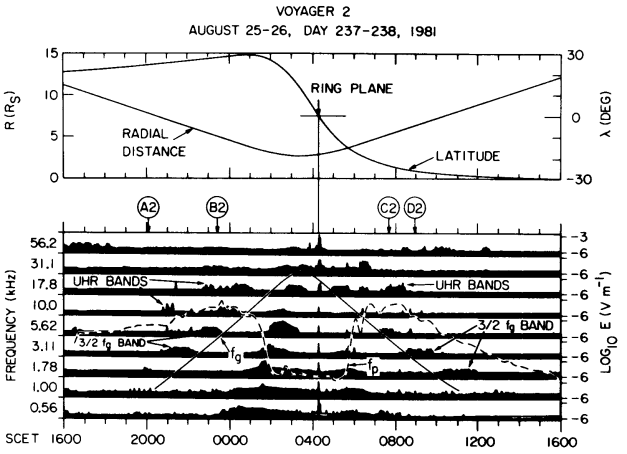

Fig. 6. An overview of Voyager 2 observations of $(n + 1/2)f_g$ emissions in the inner Saturnian magnetosphere. The 3/2 band is most prominent inside of ~8 R_S just above f_g except near closest approach when $f_p < f_g$. Some brief periods when there is a band near f_{UHR} are also apparent (see text).

As a clarifying note, we should point out that *Gurnett et al.* [1981*a*] originally identified the intense but smoothly varying emission at 31.1 kHz shortly after 0130 SCET, day 318 and seen in Figure 5 as an upper hybrid emission. This results in a significant difference in the electron density as determined by the plasma investigation [*Bridge et al.*, 1981] and the plasma wave data. *Pedersen et al.* [1981] argued the emission at 31.1 kHz was not the UHR band, but a higher harmonic. We now believe it is possible that the emission in question is likely to be at a frequency above f_{UHR}, as predicted by theoretical considerations [*Birmingham et al.*, 1981]. Birmingham et al. found that the most intense $(n + 1/2)f_g$ emission may reside in the next higher band than f_{UHR} when f_{UHR} is very close to an integral harmonic of f_g and n_c/n_h is large as is the case in the inner Saturnian magnetosphere (E. C. Sittler, Jr., private communication, 1982). Hence, if one takes this into account, f_p is in the range of 12–13 kHz and n_e is near 2 cm^{-3}, in much better agreement with the plasma observations.

The trajectory of Voyager 2 was more symmetric about the equator than that of the first encounter and the maximum latitude attained was 30° in the inner magnetosphere. As a result, the observations of the $(n + 1/2)f_g$ emissions also are much more symmetric as can be seen in Figure 6. For the second encounter, the electrostatic waves occur both during the inbound leg at local times near 15 hours as well as the outbound leg near 3 hours local time. There is no enhancement of the electron cyclotron harmonic waves near the equator. In fact, no $(n + 1/2)f_g$ emissions are observed from about 0130 to 0700 SCET, day 238 since, as can be seen by the f_p profile provided by PLS, the spacecraft traversed a low-density region where $f_p < f_g$ as the trajectory evidently took the probe outside of the plasma torus, which is observed near the equator and outside a few R_S. (We note that *Bridge et al.* [1982] speculate on densities near 100 cm^{-3} near the ring plane crossing on the basis of an analysis of the PLS ion data. Given densities of that magnitude it would be reasonable to attribute some of the wave

activity seen at 31.1 and 56.2 kHz near the Voyager 2 closest approach to $(n + 1/2)f_g$ emissions. In fact, *Warwick et al.* [1982] label some 40-kHz emissions observed near 0415 as such. Other possible identification of the emissions near the ring plane include narrowband electromagnetic radiation [*Scarf et al.*, 1982]. Reliable identification of the mode of the emissions near periapsis will have to await the final determination of the electron density.) The strong signal centered at the ring plane is the response due to dust and ice particles impacting the spacecraft [*Gurnett et al.*, 1983*a*].

As was the case for the Voyager 1 encounter, the most prominent electron cyclotron harmonic band is the 3/2 band that lies above f_g in the radial distance range of $4 \lesssim R \lesssim 8\ R_S$. Bands at higher harmonics near f_{UHR} are apparent near 2100, day 237 at 10 kHz and 2300, day 237 at 17.8 kHz on the inbound leg and near 0800, day 238 at 17.8 kHz on the outbound leg. The burst of noise near f_p (5.62 kHz) just after 1600, day 237 is evidence of either Langmuir waves at f_p or emissions similar to those shown in Figure 1. The bursty nature and limited bandwidth identifies the noise as electrostatic; however, we do not believe the emission is of the electron cyclotron harmonic type because it is isolated spatially from the inner magnetosphere where the $(n + 1/2)f_g$ bands are prominent. Unambiguous identification of the emission is probably not possible because of the lack of waveform samples with high-frequency resolution during the time period in question.

The maximum amplitudes for the $(n + 1/2)f_g$ bands are near 300 $\mu V\ m^{-1}$ and extend down to the instrument threshold of $\sim 1\ \mu V\ m^{-1}$. Typical amplitudes are 30 $\mu V\ m^{-1}$. The lowest harmonic band is consistently the strongest emission except, perhaps, for the UHR band on the Voyager 2 outbound leg at $\sim$0800 SCET, day 238. During this time, the 3/2 band is quite weak.

We were fortunate to have several high-resolution snapshots of the frequency-time spectral character of these waves that allow a more solid identification of the emissions and also provide a wealth of information that is not available in Figures 5 and 6. Figure 7 is a spectrogram obtained at 0326 SCET on day 318, 1980 during the Voyager 1 encounter. This time is noted on Figure 5 by the arrow labeled 'wideband frame.' Note that this frame was taken while Voyager 1 was still 4.5° below the equatorial plane, before the peak in the band intensity. The spectrum analyzer shows very little emission at this time, but as can be seen in Figure 7, the 3/2 band lies almost directly between the channels at 3.11 and 5.62 kHz. Evidence is also found in Figure 7 for the 5/2 band at 8 kHz and the 7/2 band at 11.5 kHz. The double-banded appearance of the 5/2 emission is due to a notch filter at 7.2 kHz in the receiver designed to filter out the third harmonic of the power supply frequency and, hence, the gap is not real.

In general, the $(n + 1/2)f_g$ bands shown in Figure 7 show little spectral structure within each of the bands, and the apparent temporal structure is probably not attributable to the natural emissions either. The disappearance of the bands at about 12-s intervals is due to intense signals at lower frequencies that decrease the gain of the automatic gain control (AGC) receiver. In this case, the low-frequency signal is interference from a stepper motor used by the low-energy charged particle experiment. Further, there are numerous sporadic bursts with broad frequency extent that give the electron cyclotron emissions a bursty appearance. These sporadic emissions are due to dust impacts [*Scarf et al.*, this issue] and, hence we do not believe all of the bursty structure is germane to the electrostatic bands in this example.

During the Voyager 2 encounter we had several more opportunities to observe the electron cyclotron harmonic emissions with high spectral and temporal resolution. Four intervals of observations are shown in Figure 8 that are taken at the

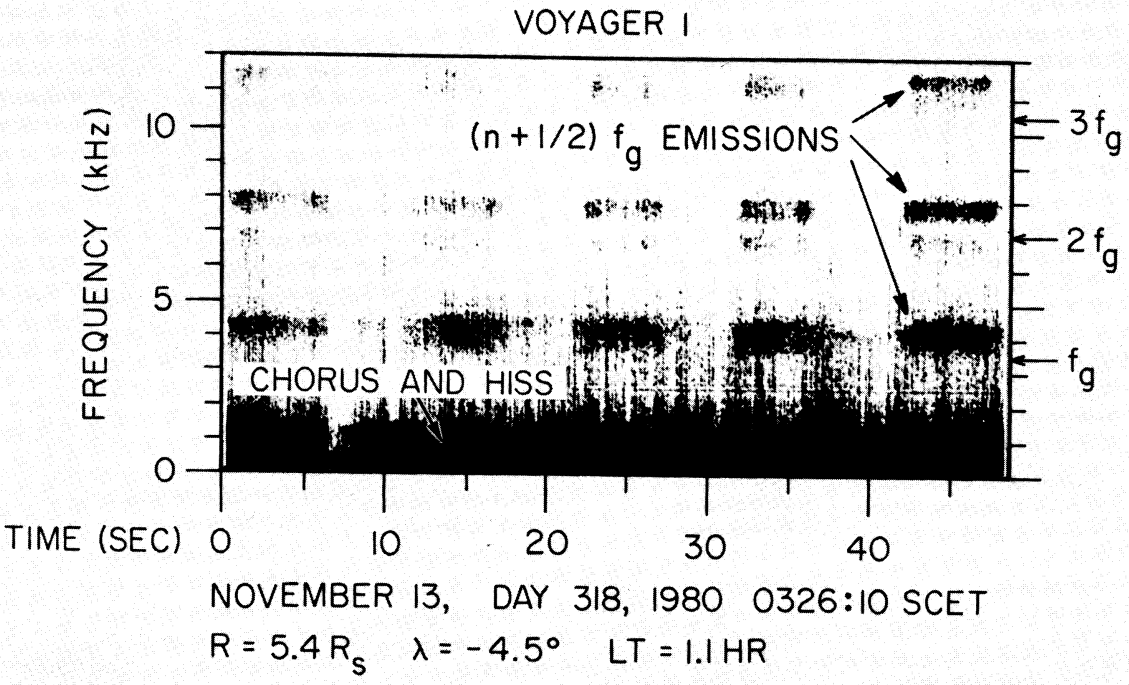

Fig. 7. A frequency-time spectrogram showing the first three harmonic bands of the $(n + 1/2)f_g$ emissions not far from the Voyager 1 outbound equator crossing near 5.4 R_S. The vertical striations visible in these emissions are not thought to be temporal variations in the bands but rather a receiver response to pulses associated with dust impacts.

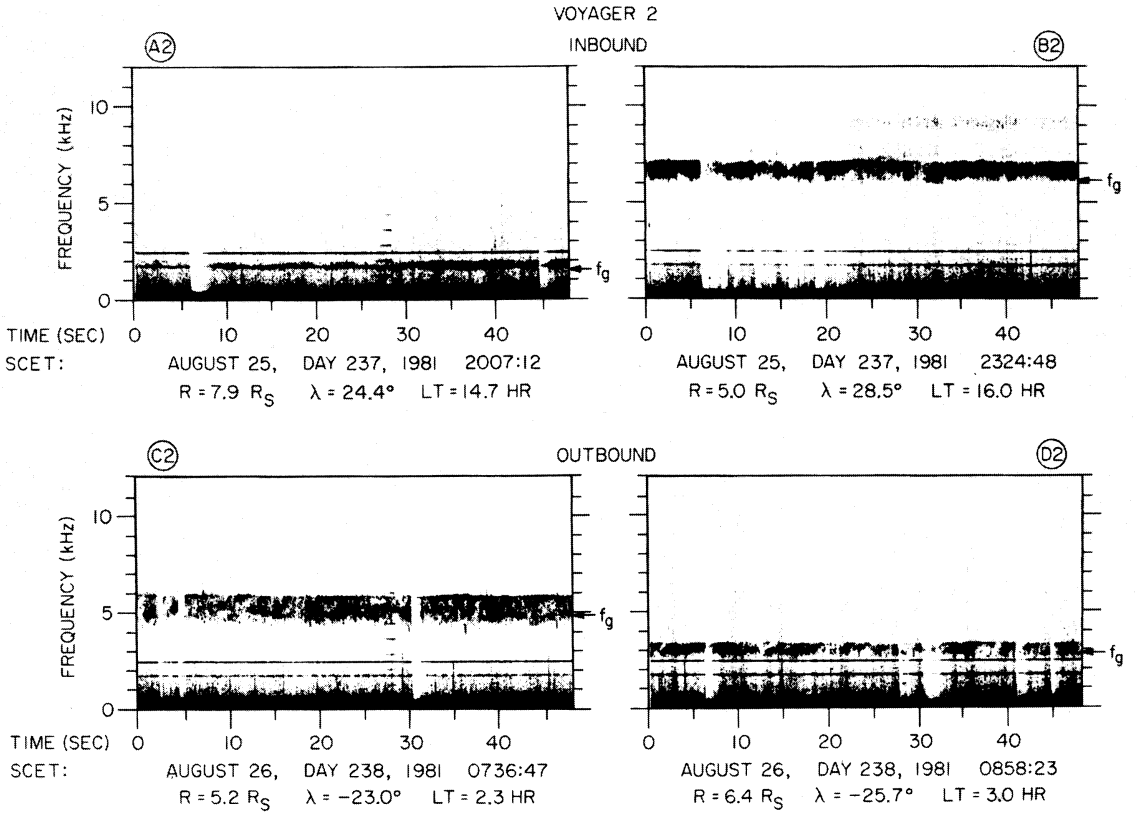

Fig. 8. Four snapshots of the 3/2 band observed by Voyager 2. Note the spectacular dynamic structure in the emission and the sharp upper frequency cutoff. The theory of *Barbosa and Kurth* [1980] gives a good first order explanation for the sharp upper-frequency cutoff.

times labeled A2, B2, C2, and D2 in Figure 6. There is no evidence of harmonic emissions in any of the bands other than the $n = 1$ band. The intermediate bands, if present, are so weak as to be undetectable and the upper hybrid emission cannot be seen even when present because it lies above the upper frequency limit for the waveform receiver.

The examples of the 3/2 band shown in Figure 8 have some striking spectral and temporal structure and display some obvious similarities from one example to the next. First, however, we should point out that the two very narrow bands near 1.75 and 2.4 kHz in each of the spectrograms are interference, as are the brief bursts at odd harmonics of 400 Hz in spectra A2 and B2. The two outbound spectra show a wealth of temporal and spectral structure, as does spectrum B2, but to a lesser extent. In some cases there appear to be drifting tones, reminiscent of chorus; however, there is no possibility these emissions are chorus because $f > f_g$. Spectra B2, C2, and D2 all have extremely sharp upper frequency cutoffs with less well-defined lower frequency limits. All bands seem to be limited by f_g on the low-frequency side except for the example in C2 that extends below f_g as determined by the onboard magnetometer (R. P. Lepping, private communication, 1982). While it is common at the earth to find the so-called 3/2 band very close to f_g[*Hubbard and Birmingham*, 1978] it is quite surprising to find the emission extending below f_g since there should be strong Landau damping at f_g and its harmonics. Another interesting trend is for the bandwidth of the emission to increase as the radial distance decreases, although $\Delta f/f$ remains approximately the same. In fact, for all the 3/2 bands shown in Figures 7 and 8 with the exception of B2, $\Delta f/f$ lies between 0.25 and 0.30. The band in B2 has $\Delta f/f \approx 0.15$.

3. Discussion

In the preceding section we have shown a variety of electrostatic wave phenomena that exist in the Saturnian magnetosphere. After the Voyager encounters with Jupiter demonstrated that most of the plasma wave phenomena (and electrostatic waves in particular) known at earth also exist in Jupiter's magnetosphere [*Scarf et al.*, 1979; *Gurnett et al.*, 1979; *Kurth et al.*, 1980*a*; *Gurnett and Scarf*, 1983] it became apparent that the instabilities involved were microinstabilities set up by distribution functions general enough in form to exist in other planetary magnetospheres, even though the magnetosphere itself could take on a grossly different macroscopic form. With this in mind, we shall compare and contrast the electrostatic wave phenomena at Saturn with those at the earth and Jupiter to try to discern how the macroscopic variations in the three magnetospheres affect the occurrence and characteristics of the emissions. Also, we shall attempt to use our understanding of the theory of electron cyclotron harmonic waves at the earth and Jupiter to make some statements about the form of the underlying distribution functions in Saturn's inner magnetosphere.

3.1. *Comparisons with Terrestrial and Jovian Electrostatic Emissions*

All of the emissions reported herein have direct terrestrial analogs, although the case is weakest for the electrostatic bursts shown in Figure 1. For these emissions we are relying almost entirely on the appearance of the dynamic spectrum for identification and have no solid evidence for the whistler mode waves that presumably trap the electrons in Landau resonance. The

actual waveforms of the electrostatic bursts do suggest the high-frequency waves are being modulated by low-frequency waves that are below $f_g/2$ and are, therefore, consistent with chorus or some other whistler mode emission.

Recently, we have uncovered evidence of similar broadband impulsive bursts at frequencies in the general vicinity of f_p in the Jovian magnetosphere, which probably strengthens the case for their presence at Saturn purely on the grounds that there now appears to be no reason to expect Saturn to be a special case. This would seem to imply that the underlying chorus waves may often act to organize enough electrons to cause a two-stream instability, if the theory of *Reinleitner et al.* [1983] is correct. We are then led to the conclusion that, if chorus is presumed to be present in the distant outer magnetospheres of Jupiter and Saturn as we know to be the case at earth, then we can expect the presence of a pitch-angle anisotropy in the electron distribution formed by the atmospheric loss cone which is thought to drive the whistler mode instability [*Kennel and Petschek*, 1966].

Langmuir waves, while they are quite prominent upstream of each of the three planetary magnetospheres, are relatively rare within the magnetospheres, themselves. There is no evidence to date of their occurrence in the Jovian magnetosphere at all. At the earth and Saturn Langmuir waves are most likely to be observed in a region where $f_p < f_g$, which probably explains their rarity since for most regions in planetary magnetospheres $f_g < f_p$. At the earth, the polar region is characterized by low densities and the occasional occurrence of plasma oscillations [*Gurnett et al.*, 1983*c*]. The example of Langmuir waves in Figure 3 was not obtained in the polar region of Saturn's magnetosphere but evidently in a low-density region either inside or above (or both) the plasma torus. Hence, the morphology of a plasma torus surrounded by a relatively low density plasma is remarkably different than that at earth. A similar low-density region may exist at Jupiter inside and above or below the Io torus, although the Voyager encounters did not traverse the proper locale to confirm its presence. The profile of f_{UHR} from the Voyager 1 Jupiter encounter [*Birmingham et al.*, 1981] is suggestive of such a region, however, in that f_{UHR} approached f_g while the spacecraft exited the torus (on the inside) in a grazing fashion.

In a general sense, the regions of occurrence of electron cyclotron harmonic emissions are quite similar in the three magnetospheres. The most intense and durable emissions occur in the inner regions of each magnetosphere. At the earth, the most prominent odd half-harmonic bands occur in the region just beyond the plasmapause. At Jupiter, $(n + 1/2)f_g$ emissions are observed within about 23 R_J [*Kurth et al.*, 1980*a*], primarily associated with the Io torus and the region just beyond. As we have seen in Figures 5 and 6, the region $R \lesssim 8\ R_S$ is a common region for the emissions of Saturn, as long as $f_p > f_g$.

The $(n + 1/2)f_g$ waves near f_{UHR} are quite common at the magnetopause at both the earth [*Kurth et al.*, 1981; R. R. Anderson and W. S. Kurth, manuscript in preparation, 1983] and Jupiter [*Gurnett et al.*, 1979, 1983*b*], although there is little evidence for them at the Saturnian magnetopause. *Scarf et al.* [1982] report weak signals at 5.6 kHz near the Voyager 2 inbound magnetopause crossing ($\sim$0700 on August 25, 1981) that they tentatively interpret as being similar to electrostatic or electromagnetic waves observed just within the magnetospheres of the earth and Jupiter, but we can only speculate that these are the UHR emissions.

The outer magnetosphere at the earth frequently shows sporadic bursts of the lower $(n + 1/2)f_g$ harmonics and sometimes those near f_{UHR}. These have not been seen in Saturn's outer magnetosphere, although with the relatively strong spacecraft interference that appears in the Voyager 1 and 2 wideband frames, it is unlikely that the lower $(n + 1/2)f_g$ bands would be visible. The emissions have only recently been discovered in Jupiter's outer magnetosphere where the low-frequency interference is not a problem. (The interference is thought to be associated with the onboard tape recorder that was used very little at Jupiter and exclusively at Saturn in recording the wideband plasma wave data [see *Scarf et al.*, this issue].) Unfortunately, the coarse frequency resolution provided by the spectrum analyzer makes it nearly impossible to differentiate between the banded emissions and other low-frequency, sporadic emissions or interference.

We noted above that there was some enhancement in the amplitude of the electron cyclotron harmonic emissions as Voyager 1 traversed Saturn's equator. The magnetic equator has been identified at earth as the most likely region for the emissions as well as being the location of the most intense bands [*Kennel et al.*, 1970; *Fredericks and Scarf*, 1973; *Gough et al.*, 1979]. At Jupiter, *Kurth et al.* [1980*a*] reported that the $(n + 1/2)f_g$ emissions were very tightly confined to the magnetic equator (within 1.9°) [see also *Barbosa and Kurth*, 1980] and that except for some diffuse electrostatic bands of much lower intensity the $(n + 1/2)f_g$ bands were not detectable at all for $|\lambda_m| > 1.9°$. In this regard, Saturn is much more like the earth since the emissions can be found in a broad range of latitudes [*Kurth et al.*, 1979] even though the most intense emissions are clustered near the magnetic equators in both magnetospheres.

We suggest the Jovian magnetosphere displays a much more pronounced latitude dependence for the occurrence of electron cyclotron harmonic waves because of the very strong rotational control of the magnetospheric dynamics due to the rapid rotation rate and substantial mass loading. These two factors lead to a highly distorted magnetic field configuration [*Connerney et al.*, 1981] in which the field lines are 'stretched' to considerably larger radial distances in the magnetic equatorial plane than in a dipole configuration. Calculation of ray paths in the magnetic meridian plane of 3/2 waves by *Barbosa and Kurth* [1980] by using a dipole field model demonstrated tight confinement to within $\pm 4°$ of the magnetic equator. Compensation for the distended field lines would increase the confinement.

3.2. *Inferences for the Electron Distribution Function*

It is not the purpose of this paper to treat the electron cyclotron harmonic emissions in a detailed theoretical study. However, it is within the scope of this survey to discuss some rudimentary points that can be made about the electron distribution functions underlying the $(n + 1/2)f_g$ emissions since a large body of theoretical work exists for the terrestrial emissions [see *Lyons*, 1974; *Ashour-Abdalla and Kennel*, 1978*a*; *Hubbard and Birmingham*, 1978; *Rönnmark et al.*, 1978, and references therein] and those at Jupiter [*Barbosa and Kurth*, 1980; *Birmingham et al.*, 1981].

The electron cyclotron harmonic waves have long been thought to be responsible for the diffusion of electrons into the loss cone, thereby providing precipitating electrons for the diffuse aurora at the earth [*Kennel et al.*, 1970; *Lyons*, 1974]. Using a quasi-linear theory, Lyons has concluded that for $L = 7$ at the earth wave amplitudes in the range of 1–10 mV m^{-1} can put electrons in the range of 1–10 keV on strong diffusion. Typical amplitudes for the 3/2 band at Saturn are

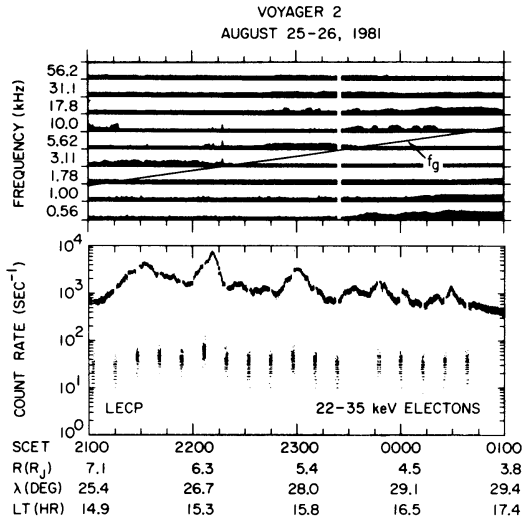

Fig. 9. Simultaneous plasma wave and LECP data showing evidence for several keV electron fluxes that may be interacting with the $(n + 1/2)f_g$ emissions seen in the upper panel (see text).

only a few tens of μV m^{-1}, hence, we doubt the $(n + 1/2)f_g$ waves at Saturn are an important factor in the energy budget of the magnetosphere. We caution the reader, however, that with only one crossing of the magnetic equator at a reasonable radial distance for the emissions (Voyager 1, outbound) our statistics are extremely poor and there may be significantly more intense waves present near the equator at other radial distances, longitudes, or times.

The current theories for the generation of the electron cyclotron harmonic waves utilize an electron distribution function with two (or more) components and are based on the Harris dispersion relation [*Harris*, 1959] for electrostatic waves propagating in a hot plasma with an imbedded magnetic field [*Ashour-Abdalla and Kennel*, 1978*a*; *Hubbard and Birmingham*, 1978; *Rönnmark et al.*, 1978]. *Young et a'l.* [1973] demonstrated that relatively weak loss-cone distributions were unstable to the electron cyclotron waves, provided a cold electron component accompanied the hotter component that possessed a free-energy source. The free-energy source apparently can take on a variety of forms [*Kurth et al.*, 1979, 1980*b*] but must have a positive slope with respect to $v_\perp$, i.e., $\partial f/\partial v_\perp > 0$.

At the earth, the free-energy source is thought to be in the range from about one to several keV [*Rönnmark et al.*, 1978; *Kurth et al.*, 1979; *Kurth et al.*, 1980*b*], hence the existence of $(n + 1/2)f_g$ emissions at Saturn may imply substantial fluxes of 1–10 keV electrons with $\partial f/\partial v_\perp > 0$. Indeed, there is some evidence for these electrons in the inner Saturnian magnetosphere. Figure 9 shows a portion of the data from Voyager 2's inbound leg presented in Figure 6 along with low-energy charged particle (LECP) observations of 22- to 35-keV electrons that are shown in the bottom panel (S. M. Krimigis, private communication, 1982). The count rates are taken from each of 8 angular sectors, one of which is shielded and provides a background count rate. The measurements taken in the shielded configuration appear approximately 5 times per hour and show rates one to two orders of magnitude smaller than those obtained in the seven unshielded sectors (see *Krimigis et al.* [1977] for details of the LECP instrumentation).

The variations observed in the count rate from the unshielded sectors probably represent temporal variations [*Krimigis et al.*, 1982, this issue]. *Krimigis et al.* [1982] analyzed the electron data shown in Figure 9 by comparing the rates in two mutually perpendicular directions and found similar intensities, suggesting a nearly isotropic pitch angle distribution. They further argued the temporal variations at energies $\lesssim 60$ keV may be evidence of electron acceleration. Although not evident in the LECP analysis, it is possible that a weak loss cone feature could be present in the energetic electrons, and we might argue that the 22- to 35-keV electrons could be the high-energy end of the spectrum of electrons responsible for driving the electron cyclotron harmonic instability. All occurrences of the $(n + 1/2)f_g$ emissions are not accompanied by the enhanced rates in the 22- to 35-keV channel; however, it is quite possible that lower energy electrons, below the LECP threshold, could drive the waves.

We can draw on the work of *Barbosa and Kurth* [1980], who studied the relation between superthermal electrons and electron cyclotron harmonic emissions in order to investigate further the electrons responsible for driving the waves. One important result of Barbosa and Kurth is that large convective growth rates in the lower portion of a harmonic band as in the case of the Saturnian 3/2 band (see Figure 8) are the result of resonant electrons having a velocity V_r only a few times the thermal speed of the cool background a. In the left-hand panel of Figure 10 we present a 4-s average spectrum from spectrum C2 in Figure 8. The frequency scale in Figure 10 is the normalized frequency $\bar{\omega} = f/f_g$. Notice that the emission is confined to the very bottom of the first harmonic band.

In the right-hand panel of Figure 10, we have recomputed the convective growth rates shown in Figure 3 of *Barbosa and Kurth* [1980] for $|V_r/a|_{\min} = 2.5$, 3, 4, and 5. The new calculations take advantage of a numerical procedure that improves the resolution and also the accuracy at low frequencies $\bar{\omega} < 1.2$ where the power law representation of the dispersion relation

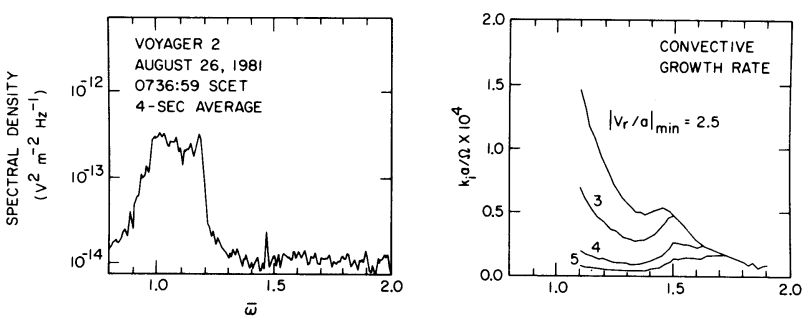

Fig. 10. A comparison of the spectrum of a typical 3/2 band observed at Saturn (left panel) with convective growth rates. Note the confinement of the Saturnian emission to the lower portion of the band between f_g and $2f_g$, $\bar{\omega} \lesssim 1.3$. This implies that $|V_r/a|_{\min}$ is small ($\lesssim 3$).

used earlier gave a perpendicular group velocity too large by a factor of 2. The overall normalization of the growth rates is also smaller by a factor of 0.24 to reflect the different parameters at Saturn. We have used here $T_{j\perp} = 1.1 \times 10^5$ cm^{-2} s^{-1} sr^{-1}, $n_c = 1.6$ cm^{-3}, and $T_c = 8$ eV for reasons described shortly. It is clear that smaller values of $|V_r/a|_{\min}$ yield growth rate curves most similar to the measured wave spectrum although we caution the reader to not make any attempt to equate spectral density with growth rate. Following Barbosa and Kurth, then, we shall choose $|V_r/a| \approx 3$. Alternately, we can say $T_R/T_c \approx 9$ where T_R and T_c refer to the temperature of the resonant electrons and cool electrons, respectively.

For a representative time on the Voyager 2 inbound leg, near 2300 SCET on August 25, $T_c \approx 8$ eV (E. C. Sittler, Jr., private communication, 1982). This implies T_R is about 70 eV. The actual value of T_R/T_c is not well specified, but it seems apparent that T_R is on the order of 100 eV and not several keV as might be suggested by the enhanced fluxes of 22- to 35-keV electrons evident in Figure 9. We conclude the electrons observed by LECP are not driving the electron cyclotron instability, although those electrons may be scattered by or perhaps even stochastically accelerated by the electrostatic waves. This conclusion is also supported by the theoretical analyses of *Ashour-Abdalla and Kennel* [1978*a*], *Hubbard and Birmingham* [1978], and *Hubbard et al.* [1979], who calculated that values of $|V_r/a| \approx 3$ were suitable for optimal growth of 3/2 emissions at earth.

We return to the plasma science measurements, then, to find evidence of fluxes of superthermal electrons with energies of 100 eV. Indeed, there is evidence for a 100- to 200-eV electron component in the same general time period with a density of ~ 0.16 cm^{-3} (E. C. Sittler, Jr., private communication, 1982). *Barbosa and Kurth* [1980] derived a quantity $T_{j\perp}{}^*(T)$ defined as the critical flux of resonant electrons able to produce 10 e foldings in amplitude of electron cyclotron waves in the Jovian magnetosphere

$$T_{j\perp}{}^*(T) = 23\left(\frac{0.1}{\delta\bar{\omega}}\right) pR^2\bar{\omega} \text{ (cm}^2\text{s sr)}^{-1} \quad (1)$$

Here, T is the electron temperature in electron volts, $\bar{\omega}$ is the wave frequency normalized to $f_g(\bar{\omega} = f/f_g)$, p is the pressure due to cool background electrons ($p = n_c T_c$) in units of eV/cm^3, and R is in planetary radii. Equation (1) can be modified for use at Saturn as follows

$$T_{j\perp}{}^*(T = T_R) = 23\left(\frac{0.1}{\delta\bar{\omega}}\right)\left(\frac{4.2G}{B_S}\right)\left(\frac{7.13 \times 10^4 \text{ km}}{R_S}\right)\left(\frac{T/T_c}{9}\right)^2 pR\bar{\omega} \quad (2)$$

B_S is the surface field magnitude at Saturn, 0.21G and R_S is 6×10^4 km. Following Barbosa and Kurth we shall choose $\bar{\omega} = 1.3$ and $\delta\bar{\omega} = 0.25$ based on the frequencies and bandwidths of the emissions in Figures 7 and 8.

We shall evaluate the expression near 2300 on day 237 where there is a UHR emission in the 17.8-kHz channel. At this time B is 174 nT [*Ness et al.*, 1982], hence, f_g is 4.87 kHz. From plasma probe measurements, $n_c = 1.6$ cm^{-3}. This would seem inconsistent with $f_{UHR} = 17.8$ kHz since $\sqrt{f_{UHR}{}^2 - f_g{}^2} = f_p = 17.1$ kHz or $n_e = 3.6$ cm^{-3}. For this calculation it is not extremely critical to have a precise value for n_c, and we shall accept the plasma probe value of 1.6 cm^{-3} simply for use in the calculation. It is important to establish that n_c/n_h is large, and this can be seen from either the plasma values (1.6/0.16) or from the plasma wave data (3.6/0.16), assuming the additional density is in the form of a plasma too cold to be detected by the plasma instrument. Proceeding, then, we can calculate $p = n_c T_c = 1.6$ cm$^{-3} \times 8$ eV $= 12.8$ eV/cm^3, and evaluating (2) gives $T_{j\perp}{}^* = 1.1 \times 10^5$ (cm^2 s sr)$^{-1}$.

The critical flux of resonant electrons from (2) can be compared with the measured flux. Given $T_h = 100$ eV and $n_h = 0.16$ cm^{-3}, the measured flux of hot electrons is 7.6×10^6 (cm^2 s sr)$^{-1}$ or 76 times greater than the critical flux. This is reassuring, and in fact, we can speculate that fluxes substantially larger than $T_{j\perp}{}^*$ are required, since Voyager is 28° off the equator where conditions for wave growth are not optimum.

Theoretical studies of various classes of electron cyclotron waves have shown some success in providing information on the electron distribution function based solely on an analysis of the wave spectrum [*Hubbard et al.*, 1979; *Birmingham et al.*, 1981]. In these studies, the waves are classified in a morphological sense such as events with only the 3/2 band, several lower $(n + 1/2)f_g$ harmonics, only emissions near f_{UHR}, etc. *Hubbard and Birmingham* [1978] published the first of these classification schemes and *Gough et al.* [1979] has added a variation. In the former scheme, each classification was described by certain plasma model parameters that yielded a computed growth rate spectrum that had features qualitatively similar to those of the observed waves. For example, the presence of only 3/2 emissions could be modeled by using a two-component plasma characterized by n_c, T_c, n_h, and T_h for the density and temperature of the cold and hot components, respectively, and setting $n_c/n_h \ll 1$ and $T_c/T_h \approx 0.1$. Similarly, the presence of a single band near f_{UHR} can be modeled with $n_c/n_h \gg 1$.

Birmingham et al. [1981] performed an analysis of $(n + 1/2)f_g$ emissions in the Io torus at Jupiter and showed T_c/T_h increases systematically from the inner edge of the torus near $L = 5$ to $L = 9$. The basis for this result was that in the inner region, only a single band near f_{UHR} was observed, while further out emissions at and above f_{UHR} were present and eventually, near $L = 9$, only harmonics at or below f_{UHR} were present. Birmingham et al. showed that these general features could be modeled by fixing $n_c/n_h \gg 1$ (since the band near f_{UHR} was always present) and varying T_c/T_h from small to larger values with increasing radial distances.

At Saturn, we might also be able to comment on the implications of the occurrence of various classes of $(n + 1/2)f_g$ emissions for the underlying electron distribution functions. The Voyager 1 observations as summarized in Figure 5 and displayed in detail in Figure 7 show multiple lower harmonic emissions, but also a band near f_{UHR} between $\sim$0300 and 0500 SCET at 56.2 and 31.1 kHz (just above f_p, as determined by PLS). The Voyager 2 observations show evidence of only the 3/2 band over most of the interval where the waves are present. For some short periods near 2100 and 2300 SCET on day 237 and near 0800 and day 238 the 3/2 band is accompanied by a higher harmonic near f_{UHR}; for these three cases $n = 5$, 3, and 3, respectively.

The presence of both the 3/2 band as well as the band near f_{UHR} implies $n_c/n_h \gg 1$ [*Ashour-Abdalla and Kennel*, 1978*b*; *Hubbard and Birmingham*, 1978]. In the regimes where the UHR band is absent, it is possible that n_c/n_h approaches 1 for the cases where multiple bands are present and less than 1 where only the 3/2 emission is present [*Hubbard and Birmingham*, 1978]. This would imply the more distant high latitude pass of Voyager 2 sampled regions where $n_c/n_h < 1$. However, it is important to consider the rather large latitude of the spacecraft and the less than ideal amplification possible there. We would argue that it is equally likely that the spacecraft remains in a

TABLE 1. Electrostatic Waves at Saturn

Type of Emission	Region	Frequency	$\Delta f/f$	Typical Amplitudes, $\mu V\ m^{-1}$
Bursts associated with chorus	Dayside, outer magnetosphere, $R \approx 16\ R_S$	$f \approx f_p \gg f_g$	10%	10
Langmuir waves	Mid-latitude inner magnetosphere $R \approx 3\ R_S$	$f = f_p \ll f_g$	3%	1000
$(n + 1/2)f_g$ bands				
$3/2\ f_g$	$4 < R < 8\ R_S$	$f \approx 1.2 f_g$	25%	30
$(n + 1/2)f_g$ $(n = 1, 2, 3)$	Equator, 5 R_S	$f_g \lesssim f \lesssim f_{UHR}$	$\Delta f_{(n+1/2)} \approx \Delta f_{3/2}$	10
$(n + 1/2)f_g \approx f_{UHR}$	$4 < R < 7\ R_S$	$f \approx f_{UHR}$	?	30

regime where $n_c/n_h \gg 1$ but that the waves fail to amplify owing to geometrical considerations [*Barbosa and Kurth*, 1980]. Indeed, plasma probe measurements give reasonably large values for n_c/n_h even at larger radial distances where the band near f_{UHR} is not present. The presence of the UHR band at smaller radial distances ($R \lesssim 6\ R_S$) implies the presence of a more dominant cold population. The Voyager 1 outbound pass is at lower latitudes and well within the plasma torus; hence, the presence of multiple harmonics plus the UHR emissions imply an even stronger influence of cold plasma. It is clear that a thorough analysis of this sort requires detailed theoretical modeling and substantial input of plasma observations available in the regions of interest, both of which are beyond the scope of this paper.

One of the most intriguing aspects of the 3/2 emissions presented herein is the dynamic structure seen in the spectrograms in Figure 8. There have been reports of rapid fluctuations in intensity of $(n + 1/2)f_g$ waves previously. For example, *Kurth et al.* [1979] reported the band near f_{UHR} showed order of magnitude fluctuations in amplitude on a time scale of a few seconds. However, very little has been done in terms of explaining the details of the fine scale temporal or spectral variations. *Barbosa and Kurth* [1980] speculated that if waves started growing with the resonant velocity V_r only slightly above the thermal speed, a, say $|V_r/a| = 2.5$, then the waves would tend to erode the loss-cone feature at the lower energies and $|V_r/a|$ would increase with time. They also showed that the effect of raising $|V_r/a|$ was to 'peel off' the growth rate at lower frequencies (as in the right-hand panel of Figure 10), resulting in a rise in the frequency of maximum growth. This implies a structure that drifts to higher frequencies with time. Even though some of the most obvious structures visible in the spectra shown in Figure 8 are rising tone features, the Barbosa and Kurth explanation probably is not correct since it would operate over time scales significantly longer than the second-long structures observed. For the present we can only conclude that inhomogeneities in the amplification region are responsible for the observed dynamic spectrum.

The sharp upper-frequency cutoff of the 3/2 band seems to follow naturally from the work of *Barbosa and Kurth* [1980], even though the spectrum at lower frequencies is complicated by the rising structures. Examination of the convective growth rates in Figure 3 of Barbosa and Kurth or the right-hand panel of Figure 10 herein shows that the effects of varying $|V_r/a|$ are seen only at lower frequencies within the band. Hence, variations in the distribution function and the resonant velocities in particular result in variations in the convective growth rate primarily at the lower frequencies. Temporal growth rates limit growth rates at the higher frequencies, therefore the upper frequency cutoff is relatively insensitive to minor variations in the form of the distribution function.

4. SUMMARY AND CONCLUSIONS

We have attempted to convey in this survey of electrostatic waves at Saturn an overview of the types of emissions present, their similarities or differences with terrestrial and Jovian analogs, and a flavor of what implications these waves have on the distribution of plasmas in the Saturnian magnetosphere. We have concentrated primarily on the electrostatic electron cyclotron harmonic emissions since they are the most prevalent electrostatic emissions in the magnetosphere. As at Jupiter, the inner and middle magnetosphere is the primary region of occurrence for the $(n + 1/2)f_g$ emissions, and they are apparently durable features of the region inside of 8 R_S, provided $f_p > f_g$. Theoretical studies of terrestrial and Jovian counterparts translate quite directly to the Saturnian environment, in apparent disregard of major differences between the gross structure of the Saturnian magnetosphere and those at Jupiter and earth.

Table 1 summarizes the electrostatic emissions found by Voyager in the Saturnian magnetosphere. The table lists the various types of emissions observed, the region where each is found, as well as the frequency of the emission with respect to the characteristic frequencies of the plasma, bandwidths, and typical amplitudes. We caution that the table is representative only of the limited observations made during the two brief encounters, and the reader should not be too quick to accept the information provided as being truly representative of the electrostatic wave spectrum in Saturn's magnetosphere.

Finally, we note that even as this initial survey of electrostatic wave phenomena at Saturn is completed, considerable work remains to be done. This survey was performed primarily from the point of view of classifying the emissions and suggesting the most viable theoretical explanation for each category on the basis of extensive work done for the earth and Jupiter. The next logical step in the study of the emissions is a unified analysis combining the plasma wave and plasma observations with a detailed theoretical analysis. Only after such a collaborative effort will there be a solid understanding of the wave-plasma interactions involved. A study of this type is currently being initiated, the results of which will be reported later.

Acknowledgments. The authors wish to express their gratitude to R. P. Lepping and the Voyager magnetometer team at Goddard Space Flight Center for magnetic field data made available for the analysis of several of the events studied herein. We are also indebted to J. D. Scudder and E. C. Sittler, Jr., of the Voyager plasma science team for the use of unpublished electron data used in this paper. We thank S. M.

Krimigis and J. F. Carbary for the use and interpretation of the LECP electron data presented in Figure 9. The authors wish, also, to thank L. A. Reinleitner for several enlightening discussions. The research at the University of Iowa was supported by the National Aeronautics and Space Administration through contract 954013 with the Jet Propulsion Laboratory and grant NGL-16-001-043 from NASA Headquarters. The research at TRW was supported by NASA through contract 954012 with the Jet Propulsion Laboratory. The research at UCLA was supported by NASA through grant NGL-05-007-190.

The Editor thanks B. M. Pedersen and R. F. Hubbard for their assistance in evaluating this paper.

REFERENCES

Ashour-Abdalla, M., and C. F. Kennel, Nonconvective and convective electron cyclotron harmonic instabilities, *J. Geophys. Res.*, *83*, 1531, 1978*a*.

Ashour-Abdalla, M., and C. F. Kennel, Multi-harmonic electron cyclotron instabilities, *Geophys. Res. Lett.*, *5*, 711, 1978*b*.

Barbosa, D. D., and W. S. Kurth, Superthermal electrons and Bernstein waves in Jupiter's inner magnetosphere, *J. Geophys. Res.*, *85*, 6729, 1980.

Birmingham, T. J., J. K. Alexander, M. D. Desch, R. F. Hubbard, and B. M. Pedersen, Observations of electron gyroharmonic waves and the structure of the Io torus, *J. Geophys. Res.*, *86*, 8497, 1981.

Bridge, H. S., F. Bagenal, J. W. Belcher, A. J. Lazarus, R. L. McNutt, J. D. Sullivan, P. R. Gazis, R. E. Hartle, K. W. Ogilvie, J. D. Scudder, E. C. Sittler, A. Eviatar, G. L. Siscoe, C. K. Goertz, and V. M. Vasyliunas, Plasma observations near Saturn: Initial results from Voyager 2, *Science*, *215*, 563, 1982.

Bridge, H. S., J. W. Belcher, A. J. Lazarus, S. Olbert, J. D. Sullivan, F. Bagenal, P. R. Gazis, R. E. Hartle, K. W. Ogilvie, J. D. Scudder, E. C. Sittler, A. Eviatar, G. L. Siscoe, C. K. Goertz, and V. M. Vasyliunas, Plasma observations near Saturn: Initial results from Voyager 1, *Science*, *212*, 217, 1981.

Connerney, J. E. P., M. H. Acuña, and N. F. Ness, Modeling the Jovian current sheet and inner magnetosphere, *J. Geophys. Res.*, *86*, 8370, 1981.

Fredricks, R. W., and F. L. Scarf, Recent studies of magnetospheric electric field emissions above the electron gyrofrequency, *J. Geophys. Res.*, *78*, 310, 1973.

Gough, M. P., P. J. Christiansen, G. Martelli, and E. J. Gershuny, Interaction of electrostatic waves with warm electrons at the geomagnetic equator, *Nature*, *279*, 515, 1979.

Gurnett, D. A., and F. L. Scarf, Plasma waves in the Jovian magnetosphere, in *Physics of the Jovian Magnetosphere*, edited by A. J. Dessler, p. 285, Cambridge University Press, New York, 1983.

Gurnett, D. A., W. S. Kurth, and F. L. Scarf, Plasma wave observations near Jupiter: Initial results from Voyager 2, *Science*, *206*, 987, 1979.

Gurnett, D. A., W. S. Kurth, and F. L. Scarf, Plasma waves near Saturn: Initial results from Voyager 1, *Science*, *212*, 235, 1981*a*.

Gurnett, D. A., W. S. Kurth, and F. L. Scarf, Narrowband electromagnetic emissions from Saturn's magnetosphere, *Nature*, *292*, 733, 1981*b*.

Gurnett, D. A., J. E. Maggs, D. L. Gallagher, W. S. Kurth, and F. L. Scarf, Parametric interaction and spatial collapse of beam-driven Langmuir waves in the solar wind, *J. Geophys. Res.*, *86*, 8833, 1981*c*.

Gurnett, D. A., E. Grün, D. Gallagher, W. S. Kurth, and F. L. Scarf, Micron-size particles detected near Saturn by the Voyager plasma wave instrument, *Icarus*, in press, 1983*a*.

Gurnett, D. A., W. S. Kurth, and F. L. Scarf, Narrowband electromagnetic emissions from Jupiter's magnetosphere, *Nature*, in press, 1983*b*.

Gurnett, D. A., S. D. Shawhan, and R. R. Shaw, Auroral hiss, Z mode radiation and auroral kilometric radiation in the polar magnetosphere: DE-1 observations, *J. Geophys. Res.*, *88*, 329, 1983*c*.

Harris, E. G., Unstable plasma oscillations in a magnetic field, *Phys. Rev. Lett.*, *2*, 34, 1959.

Hubbard, R. F., and T. J. Birmingham, Electrostatic emissions between electron gyroharmonics in the outer magnetosphere, *J. Geophys. Res.*, *83*, 4837, 1978.

Hubbard, R. F., T. J. Birmingham, and E. W. Hones, Jr., Magnetospheric electrostatic emissions and cold plasma densities, *J. Geophys. Res.*, *84*, 5828, 1979.

Kennel, C. F., and H. E. Petschek, Limit on stably trapped particle fluxes, *J. Geophys. Res.*, *71*, 1, 1966.

Kennel, C. F., F. L. Scarf, R. W. Fredricks, J. H. McGehee, and F. V. Coroniti, VLF electric field observations in the magnetosphere, *J. Geophys. Res.*, *75*, 6136, 1970.

Krimigis, S. M., T. P. Armstrong, W. I. Axford, C. O. Bostrom, C. Y. Fan, G. Gloeckler, and L. J. Lanzerotti, The low energy charged particle (LECP) experiment on the Voyager spacecraft, *Space Sci. Rev.*, *21*, 329, 1977.

Krimigis, S. M., T. P. Armstrong, W. I. Axford, C. O. Bostrom, G. Gloeckler, E. P. Keath, L. J. Lanzerotti, J. F. Carbary, D. C. Hamilton, and E. C. Roelof, Low-energy hot plasma and particles in Saturn's magnetosphere, *Science*, *215*, 571, 1982.

Krimigis, S. M., J. F. Carbary, E. P. Keath, T. P. Armstrong, L. J. Lanzerotti, and G. Gloeckler, General characteristics of hot plasma and energetic particles in the Saturnian magnetosphere: Results from the Voyager spacecraft, *J. Geophys. Res.*, this issue.

Kurth, W. S., J. D. Craven, L. A. Frank, and D. A. Gurnett, Intense electrostatic waves near the upper hybrid resonance frequency, *J. Geophys. Res.*, *84*, 4145, 1979.

Kurth, W. S., D. D. Barbosa, D. A. Gurnett, and F. L. Scarf, Electrostatic waves in the Jovian magnetosphere, *Geophys. Res. Lett.*, *7*, 57, 1980*a*.

Kurth, W. S., L. A. Frank, M. Ashour-Abdalla, D. A. Gurnett, and B. G. Burek, Observations of a free-energy source for intense electrostatic waves, *Geophys. Res. Lett.*, *7*, 293, 1980*b*.

Kurth, W. S., D. A. Gurnett, and R. R. Anderson, Escaping nonthermal continuum radiation, *J. Geophys. Res.*, *86*, 5519, 1981.

Lyons, L. R., Electron diffusion driven by magnetospheric electrostatic waves, *J. Geophys. Res.*, *79*, 575, 1974.

Ness, N. F., M. H. Acuña, R. P. Lepping, J. E. P. Connerney, K. W. Behannon, L. F. Burlaga, and F. M. Neubauer, Magnetic field studies by Voyager 1: Preliminary results at Saturn, *Science*, *212*, 211, 1981.

Ness, N. F., M. H. Acuña, K. W. Behannon, L. F. Burlaga, J. E. P. Connerney, R. P. Lepping, and F. M. Neubauer, Magnetic field studies by Voyager 2: Preliminary results at Saturn, *Science*, *215*, 558, 1982.

Pedersen, B. M., M. G. Aubier, and J. K. Alexander, Low-frequency plasma waves near Saturn, *Nature*, *292*, 714, 1981.

Reinleitner, L. A., D. A. Gurnett, and D. L. Gallagher, Chorus-related electrostatic bursts in the earth's outer magnetosphere, *Nature*, *295*, 46, 1982.

Reinleitner, L. A., D. A. Gurnett, and T. E. Eastman, Electrostatic bursts generated by electrons in Landau resonance with whistler mode chorus, *J. Geophys. Res.*, in press, 1983.

Rönnmark, K., H. Borg, P. J. Christiansen, M. P. Gough, and D. Jones, Banded electron cyclotron harmonic instability—A first comparison of theory and experiment, *Space Sci. Rev.*, *22*, 401, 1978.

Scarf, F. L., and D. A. Gurnett, A plasma wave investigation for the Voyager mission, *Space Sci. Rev.*, *21*, 289, 1977.

Scarf, F. L., D. A. Gurnett, and W. S. Kurth, Jupiter plasma wave observations: An initial Voyager 1 overview, *Science*, *204*, 991, 1979.

Scarf, F. L., D. A. Gurnett, W. S. Kurth, and R. L. Poynter, Voyager 2 plasma wave observations at Saturn, *Science*, *215*, 587, 1982.

Scarf, F. L., D. A. Gurnett, W. S. Kurth, and R. L. Poynter, Voyager plasma wave measurements at Saturn, *J. Geophys. Res.*, this issue.

Warwick, J. W., D. R. Evans, J. H. Romig, J. K. Alexander, M. D. Desch, M. L. Kaiser, M. Aubier, Y. Leblanc, A Lecacheux, and B. M. Pedersen, Planetary radio astronomy observations from Voyager 2 near Saturn, *Science*, *215*, 582, 1982.

Young, T. S. T., J. D. Callen, and J. E. McCune, High-frequency electrostatic waves in the magnetosphere, *J. Geophys. Res.*, *78*, 1082, 1973.

(Received November 29, 1982;
revised February 22, 1983;
accepted February 23, 1983.)